J Physiol 593.12 (2015) pp 2649–2663

The Journal of Physiology

Regulation of calcium clock-mediated pacemaking by inositol-1,4,5-trisphosphate receptors in mouse sinoatrial nodal cells

Nidhi Kapoor[1], Andrew Tran[1], Jeanney Kang[1], Rui Zhang[1], Kenneth D. Philipson[2] and Joshua I. Goldhaber[1]

[1] *Heart Institute, Cedars-Sinai Medical Center, Los Angeles, California, USA*
[2] *Department of Physiology, David Geffen School of Medicine at University of California Los Angeles, Los Angeles, California, USA*

Key points

- Inositol-1,4,5-trisphosphate receptors (IP_3Rs) modulate pacemaking in embryonic heart, but their role in adult sinoatrial node (SAN) pacemaking is uncertain.
- We found that stimulation of IP_3Rs accelerates spontaneous pacing rate in isolated mouse SAN cells, whereas inhibition of IP_3Rs slows pacing.
- In atrial-specific sodium-calcium exchanger (NCX) knockout (KO) SAN cells, where the Ca^{2+} clock is uncoupled from the membrane clock, IP_3R agonists and antagonists modulate the rate of spontaneous Ca^{2+} waves, suggesting that IP_3R-mediated Ca^{2+} release modulates the Ca^{2+} clock.
- IP_3R modulation also regulates Ca^{2+} spark parameters, a reflection of ryanodine receptor open probability, consistent with the effect of IP_3 signalling on Ca^{2+} clock frequency.
- Modulation of Ca^{2+} clock frequency by IP_3 signalling in NCX KO SAN cells demonstrates that the effect is independent of NCX.
- These findings support development of IP_3 signalling modulators for regulation of heart rate, particularly in heart failure where IP_3Rs are upregulated.

Abstract Cardiac pacemaking initiated by the sinus node is attributable to the interplay of several membrane currents. These include the depolarizing 'funny current' (I_f) and the sodium-calcium exchanger current (I_{NCX}). The latter is activated by ryanodine receptor (RyR)-mediated calcium (Ca^{2+}) release from the sarcoplasmic reticulum (SR). Another SR Ca^{2+} release channel, the inositol-1,4,5-triphosphate receptor (IP_3R), has been implicated in the generation of spontaneous Ca^{2+} release in atrial and ventricular cardiomyocytes. Whether IP_3R-mediated Ca^{2+} release also influences SAN automaticity is controversial, in part due to the confounding influence of periodic Ca^{2+} flux through the sarcolemma accompanying each beat. We took advantage of atrial-specific sodium–calcium exchanger (NCX) knockout (KO) SAN cells to study the influence of IP_3 signalling on cardiac pacemaking in a system where periodic intracellular Ca^{2+} cycling persists despite the absence of depolarization or Ca^{2+} flux across the sarcolemma. We recorded confocal line scans of spontaneous Ca^{2+} release in WT and NCX KO SAN cells in the presence or absence of an IP_3R blocker (2-aminoethoxydiphenyl borate, 2-APB), or during block of IP_3 production by the phospholipase C inhibitor U73122. 2-APB and U73122 decreased the frequency of spontaneous Ca^{2+} transients and waves in WT and NCX KO cells, respectively. Alternatively, increased IP_3 production induced by phenylephrine increased Ca^{2+} transient and wave frequency. We conclude that IP_3R-mediated SR Ca^{2+} flux is crucial for initiating and modulating the RyR-mediated Ca^{2+} cycling that regulates SAN pacemaking. Our results in NCX KO SAN cells also demonstrate that RyRs, but not NCX, are required for IP_3 to modulate Ca^{2+} clock frequency.

DOI: 10.1113/JP270082

(Received 16 December 2014; accepted after revision 15 April 2015; first published online 22 April 2015)
Corresponding author J. I. Goldhaber: Cedars-Sinai Heart Institute, Davis 1017, 8700 Beverly Blvd, Los Angeles, CA 90048, USA. Email: goldhaberj@cshs.org

Abbreviations AP, action potential; 2-APB, 2-aminoethoxydiphenyl borate; $[Ca]_i$, cytosolic free Ca^{2+} concentration; DAG, diacylglycerol; HCN4, hyperpolarization activated cyclic nucleotide-gated cation channel 4; I_f, funny current; I_{NCX}, sodium–calcium exchanger current; IP_3, inositol-1,4,5-trisphosphate; IP_3R, IP_3 receptor; LCC, L-type Ca^{2+} channel; LCR, local Ca^{2+} release; NCX, sodium–calcium exchanger; PE, phenylephrine; PIP_2, phosphatidylinositol (4,5)-bisphosphate; P_o, open probability; Ry, ryanodine; RyR, ryanodine receptor; SAN, sinoatrial node; SERCA, sarcoplasmic/endoplasmic reticulum Ca^{2+} ATPase; SR, sarcoplasmic reticulum; TET, tetracaine.

Introduction

The primary cardiac pacemaker resides in the sinoatrial node (SAN). Specialized SAN pacemaker cells generate ionic currents that contribute to diastolic depolarization until the membrane potential reaches the threshold for L-type Ca^{2+} channels (LCCs) to open and produce an action potential (AP). Two 'clocks' drive pacemaker activity in the SAN: the 'membrane clock' and the 'Ca^{2+} clock'. The 'membrane clock' uses ion channels in the membrane, most notably the funny current (I_f) through hyperpolarization activated cyclic nucleotide-gated cation channel 4 (HCN4), to drive diastolic depolarization (DiFrancesco, 1995). The 'Ca^{2+} clock' uses periodic ryanodine receptor (RyR)-mediated Ca^{2+} release from the sarcoplasmic reticulum (SR) to drive SAN automaticity (Lipsius *et al.* 2001; Lakatta *et al.* 2003, 2006; Lipsius & Bers, 2003; Vinogradova *et al.* 2004). This local Ca^{2+} release (LCR) by RyRs leads to a depolarizing current carried by the electrogenic sodium–calcium exchanger (NCX) as it removes cytoplasmic Ca^{2+} (Vinogradova *et al.* 2006). In addition to RyRs, several lines of evidence suggest that Ca^{2+} flux through inositol 1,4,5-trisphosphate receptors (IP_3Rs) on the SR may play a modulatory role in cardiac pacemaking (Bramich *et al.* 2001; Ju *et al.* 2011; Ju *et al.* 2012). While both the membrane and the Ca^{2+} clock mechanisms have been extensively investigated, the role of IP_3Rs in pacemaking remains poorly understood. This may be of particular importance in the setting of heart failure where IP_3R expression in the SAN is increased and HCN4 expression is decreased (Verkerk *et al.* 2003; Zicha *et al.* 2005; Yanni *et al.* 2011; Ju *et al.* 2012).

Studying the effects of IP_3 signalling on intracellular Ca^{2+} and pacemaking can be challenging because of the confounding influence of periodic Ca^{2+} flux through the sarcolemma with every beat. In addition, pharmacological blockers of ion channels and transporters are often non-specific (Bootman *et al.* 2002; Reuter *et al.* 2002; Brustovetsky *et al.* 2011; Abramochkin & Vornanen, 2014; Wiczer *et al.* 2014). To avoid these confounders, we took advantage of the atrial-specific NCX KO mouse where the entire atrium and SAN lack NCX (Groenke *et al.* 2013). NCX KO SAN cells are healthy with intact I_f and preserved SR Ca^{2+} stores (Groenke *et al.* 2013). Although these cells exhibit the periodic intracellular Ca^{2+} release events (Ca^{2+} waves and Ca^{2+} sparks) indicative of a functioning Ca^{2+} clock, they lack spontaneous action potentials (Groenke *et al.* 2013). This is because the Ca^{2+} clock is 'uncoupled' from the membrane due to the absence of NCX. Ca^{2+} flux across the sarcolemmal membrane is therefore practically eliminated (i.e. no NCX, and insignificant Ca^{2+} flux through LCCs due to lack of depolarization). Nevertheless, intracellular Ca^{2+} release events occur at a similar frequency to the spontaneous Ca^{2+} transients observed in WT SAN cells (Groenke *et al.* 2013). Using this system, we found that IP_3 signalling modulates RyRs and thus pacemaker rate by influencing the 'Ca^{2+} clock' mechanism of SAN pacemaking.

Methods

Ethical approval

This study was carried out in strict accordance with the recommendations in the *Guide for the Care and Use of Laboratory Animals* of the National Institutes of Health. All mouse experiments were approved by the Institutional Animal Care and Use Committee at Cedars-Sinai Medical Center (IACUC #: 003574). We anaesthetized the mice with isoflurane prior to heart removal.

Isolation of SAN myocytes from adult mouse hearts

We enzymatically isolated murine SAN cells from 8- to 12-week-old, male and female $NCX^{fx/fx}$ mice (referred to throughout as wild type or WT) and atrial-specific NCX KO mice using an established protocol (Groenke *et al.* 2013). Following isolation, we plated the cells on laminin-coated glass bottom Petri dishes, and used the cells within 6 h of isolation, the time frame during which

the cells were healthy and viable based on trypan blue staining and stable rhythmic beating.

Ca^{2+} measurements and confocal microscopy

We measured $[Ca^{2+}]_i$ using the Ca^{2+}-sensitive indicator Cal-520/AM (AAT Bioquest, Sunnyvale, CA, USA). Cal-520 is a BAPTA-based Ca^{2+} indicator that has a higher signal to noise ratio than Fluo-4 (Tada *et al.* 2014). Consequently we were able to use lower concentrations of dye to avoid buffering. We loaded cells previously plated on laminin-coated glass bottom dishes with Cal-520/AM (0.5 μM) dissolved in a modified tyrodes solution for 45 min at 20–22°C, followed by a 15 min wash in dye-free tyrodes. The tyrodes solution, which we also used to perfuse cells throughout experiments, contained (in mM): NaCl 140; KCl 5.4; $CaCl_2$ 1.5; $MgCl_2$ 1.5; glucose 10; Hepes 5 (pH adjusted to 7.4 with NaOH). We carried out these experiments at room temperature (20–22°C). We used the line scan mode of a Leica TCS-SP5-II confocal microscope (Leica Microsystems, Wetzlar, Germany) to perform spatiotemporal recordings of $[Ca^{2+}]_i$ (Chantawansri *et al.* 2008; Groenke *et al.* 2013). The dye was excited at 488 nm and fluorescence emission light was collected at >515 nm. We used a 63× water objective lens (Leica: HCX OL APO 63×/1.20W CORR CS), and a line scan frequency of 400 Hz. Fluorescence (F) was ratioed to baseline (F_0) after background subtraction. We used ImageJ 1.34 (Schneider *et al.* 2012) and GraphPad Prism 4 software (La Jolla, CA, USA) to analyse the image data. We also used SparkMaster (Picht *et al.* 2007) to detect and analyse Ca^{2+} sparks in our images. The spontaneous Ca^{2+} transient frequency in WT SAN cells was stable for 6 min, the maximum time course for experiments included in this study.

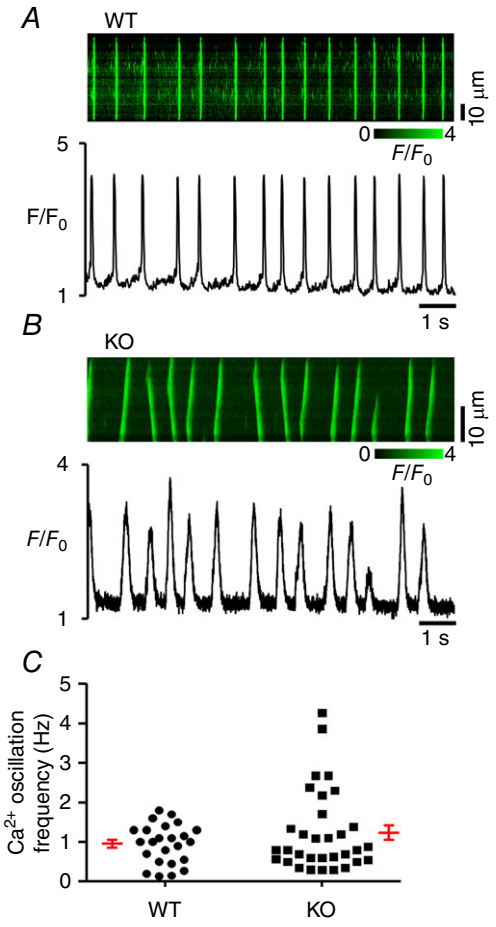

Figure 1. Ca^{2+} oscillations in WT and NCX KO SAN cells
A and *B*, confocal linescan images and corresponding fluorescence intensity plots of a representative WT SAN cell (*A*), and a representative NCX KO SAN cell (*B*). *C*, summary plots of Ca^{2+} oscillation frequency in WT SAN cells (transients; n =24 cells) and NCX KO SAN cells (waves; n =32 cells). Lines in each plot indicate the mean frequency ± SEM. P = n.s., unpaired Student's t-test.

Chemicals

All chemicals including phenylephrine (PE), caffeine, tetracaine (TET) and 2-aminoethoxydiphenyl borate (2-APB) were purchased from Sigma-Aldrich (St. Louis, MO, USA). We purchased ryanodine (Ry), U73122 and U73343 from Tocris Biosciences (Bristol, UK).

Immunocytochemistry

We fixed SAN cells with 4% paraformaldehyde and permeabilized them with 0.1% Triton X-100. We then incubated the cells with the appropriate primary antibody as follows: rabbit anti-HCN4 (abcam (ab69054); 1:500), mouse anti-α-sarcomeric actin (Sigma (A2172); 1:400) rabbit anti-IP$_3$R2 (Abcam Inc., Cambridge, MA, USA (ab5805); 1:100). Secondary antibodies used were goat anti-rabbit Alexa 488 or goat anti-mouse Alexa 568 (Invitrogen, Carlsbad, CA, USA; A-11034 and A-11031; 1:1000).

Statistics

Results are presented as mean ± SEM and n is the number of experiments. Statistical differences were determined by Student's t-test or one-way ANOVA with Holm–Sidak's multiple comparisons test and considered significant at $P < 0.05$.

Results

Periodic $[Ca^{2+}]_i$ cycling in NCX KO SAN cells

Enzymatically isolated NCX KO SAN cells have no spontaneous APs or Ca^{2+} transients, but they do display periodic Ca^{2+} sparks suggestive of Ca^{2+} clock activity

(Groenke *et al.* 2013). We confirmed this result using a high efficiency Ca^{2+} dye (0.5 μM of the Ca^{2+} indicator Cal-520/AM (Tada *et al.* 2014)) to examine Ca^{2+} cycling. WT SAN cells displayed rapid upstroke Ca^{2+} transients, indicative of depolarization, at the typical published rate (Groenke *et al.* 2013; Herrmann *et al.* 2013) (Fig. 1*A* and *C*). NCX KO SAN cells had no Ca^{2+} transients, but instead exhibited periodic Ca^{2+} sparks and Ca^{2+} waves at frequencies similar to WT (Fig. 1*B* and *C*). Previously we had only observed Ca^{2+} sparks when using Fluo 4, suggesting that the low concentration of Cal-520 avoids Ca^{2+} buffering. The similarity in frequency between WT Ca^{2+} transients and KO Ca^{2+} sparks and waves is consistent with NCX KO cells possessing a functioning Ca^{2+} clock that is 'uncoupled' from the membrane, as we reported previously (Groenke *et al.* 2013). To exclude the possibility that overload of SR Ca^{2+} stores was responsible for the Ca^{2+} waves in KO cells, we recorded Ca^{2+} release in response to application of caffeine (20 mM). Caffeine releases all Ca^{2+} from the SR, and the amplitude of the caffeine-induced transient is an indicator of SR Ca^{2+} content. We found no difference in the amplitude of the caffeine-induced transients between WT and NCX KO SAN cells (Fig. 2*A*–*C*), indicating similar SR Ca^{2+} stores in both WT and KO.

Blocking IP_3Rs inhibits intracellular Ca^{2+} Cycling

Ju *et al.* (2011) previously identified IP_3Rs in the murine SAN and also reported that IP_3 signalling could

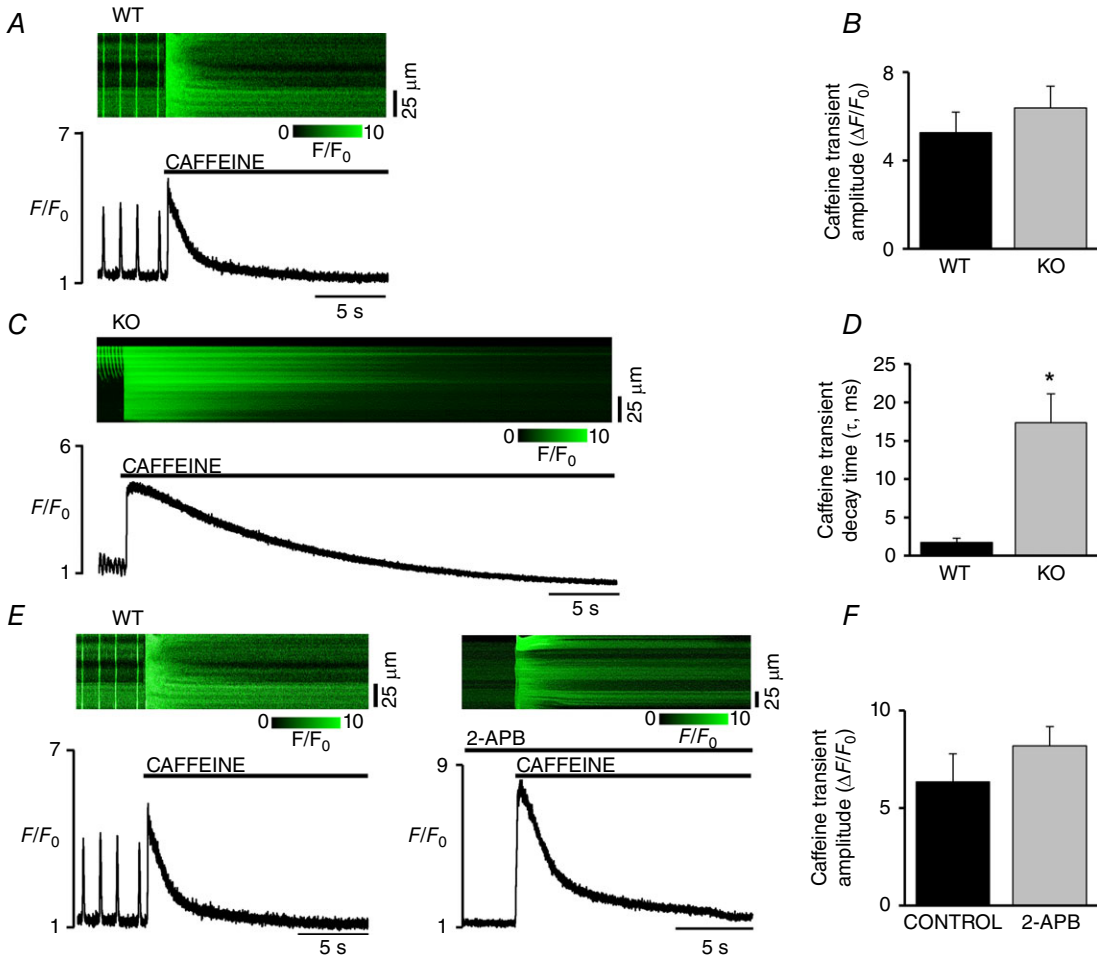

Figure 2. Caffeine releasable SR Ca^{2+} stores
A and *C*, confocal linescan images and corresponding fluorescence intensity plots of a representative WT (*A*) and an NCX KO SAN cell (*C*) during application of 20 mM caffeine. *B*, pooled data showing no significant difference in caffeine-induced Ca^{2+} transient amplitude in WT (n =8) and NCX KO SAN cells (n =5). *D*, Ca^{2+} transient decay (τ) was markedly slowed in NCX KO SAN cells, consistent with the absence of NCX. *E*, representative confocal linescan images and corresponding fluorescence intensity plots showing caffeine-induced Ca^{2+} transients in a WT SAN cell under control conditions (left) and another WT SAN cell during superfusion with 2-APB (right). *F*, summary plots showing no significant difference in the caffeine-induced Ca^{2+} transient amplitude in control conditions (n =8) and in 2-APB (n =10). *$P < 0.05$, unpaired Student's t-test.

alter pacemaker frequency. However, the expression and distribution of IP_3Rs in SAN cells isolated from NCX KO SAN is not known. Using immunocytochemistry, we confirmed that IP_3Rs were present in NCX KO SAN cells, with a similar cellular distribution to IP_3Rs in WT SAN cells (Fig. 3).

We then tested the effects of the widely used IP_3R blocker, 2-APB, on spontaneous Ca^{2+} transients in SAN cells. We used a low concentration of 2-APB (2 μM) that is known to block IP_3R-mediated Ca^{2+} release in ventricular myocytes without affecting evoked Ca^{2+} transients (Peppiatt *et al.* 2003; Kapur & Banach, 2007). This is also a much lower concentration than what has been used in previous studies examining the role of IP_3Rs on SAN pacing (Bramich *et al.* 2001; Ju *et al.* 2011). We found that 2-APB led to an 82.7% decrease (from 1.92 ± 0.32 to 0.33 ± 0.22 Hz; $n = 9$, $P < 0.05$) in the frequency of Ca^{2+} transients (Fig. 4*A* and *C*), without depleting RyR-mediated intracellular Ca^{2+} stores (Fig. 2*E* and *F*). In 7 of the 9 cells tested, Ca^{2+} transients were completely abolished by 2-APB. These results suggest that IP_3R-mediated Ca^{2+} release is required for SAN pacemaking.

Although 2-APB (2 μM) is reportedly specific for IP_3Rs (Peppiatt *et al.* 2003; Kapur & Banach, 2007), we cannot exclude the possibility that 2-APB has non-specific effects on the interplay between LCCs, NCX, RyRs or even I_f that might also retard pacemaking. Therefore, we repeated this experiment using NCX KO SAN cells where the Ca^{2+} clock is still functioning but is 'uncoupled' from the plasma membrane. In NCX KO SAN cells, blocking IP_3Rs with 2-APB led to a $64.3 \pm 7.5\%$ decrease ($n = 9$) in the frequency of spontaneous Ca^{2+} waves (Fig. 4*B* and *D*; $P < 0.05$), similar to the reduction in the frequency of depolarization-associated Ca^{2+} transients in WT cells. There was no change in caffeine-releasable SR Ca^{2+} content after 2-APB in the SAN cells that could explain the reduction in Ca^{2+} oscillation frequency. These results are consistent with direct effects of IP_3Rs on the Ca^{2+} clock. We also found that 2-APB had no effect on the velocity of Ca^{2+} wave propagation in NCX KO SAN cells, suggesting that IP_3R-mediated Ca^{2+} release is crucial for

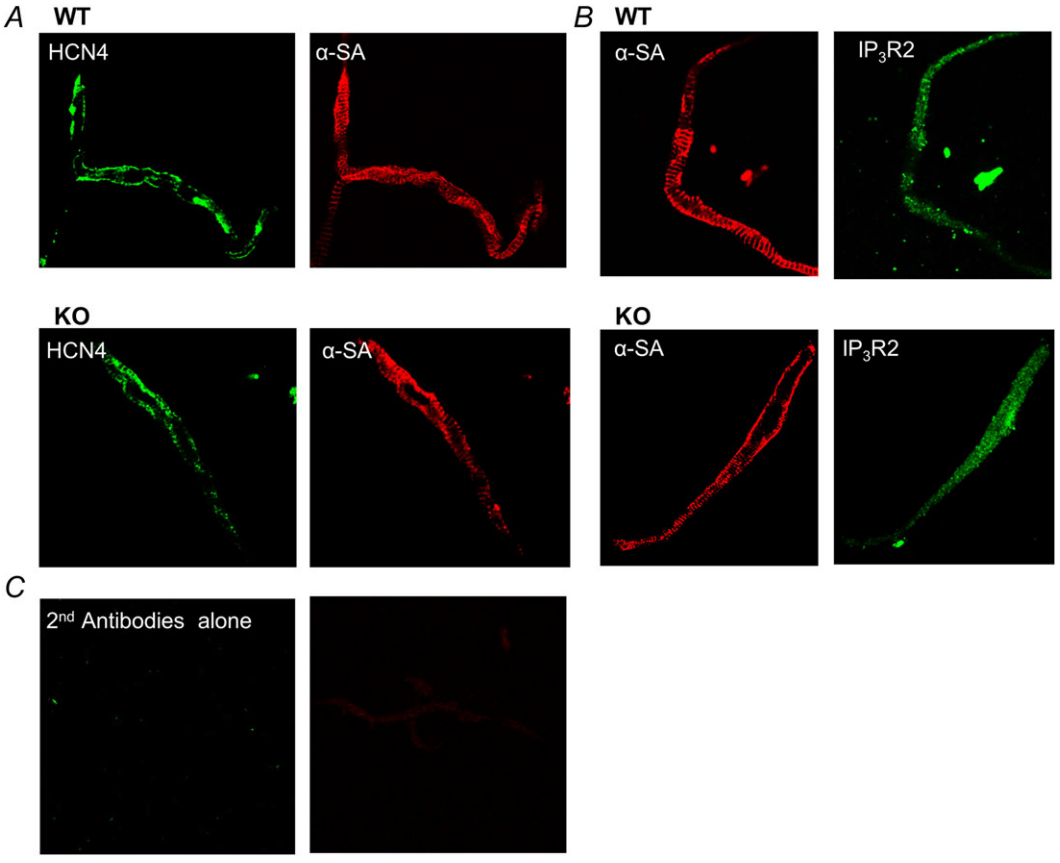

Figure 3. Immunostaining of SAN cells with antibodies against HCN4, α-sarcomeric actin and IP_3R2
A, HCN4 and α-sarcomeric actin staining of WT and NCX KO SAN cells confirm the cardiac pacemaker phenotype of these cells. *B*, α-sarcomeric actin (α-SA) and IP_3R2 staining of WT and NCX KO SAN cells show similar IP_3R2 distribution in NCX KO SAN cells and WT SAN cells. *C*, co-immunostaining of a WT SAN cell with only the secondary antibodies. The signal for the secondary antibodies could not be detected, confirming the specificity of the primary antibodies used.

the initiation of the Ca^{2+} waves but has no significant effect on their propagation velocity.

Modulation of pacing rate by phospholipase C

Phospholipase C (PLC) activation generates IP_3 that ultimately binds to IP_3Rs to release Ca^{2+} from intracellular stores. Conversely, inhibition of PLC decreases IP_3 levels. We hypothesized that inhibition of PLC would reduce IP_3 and thus slow pacing and Ca^{2+} oscillation frequency similar to the IP_3R blocker 2-APB. To test this hypothesis, we superfused WT and KO cells with the PLC antagonist U73122. Similar to IP_3R blockade with 2-APB, inhibition of PLC by U73122 (1 μM) suppressed spontaneous Ca^{2+} transient frequency in WT SAN cells by 80.8 $\pm$ 11.8% (Fig. 5*A* and *B*, n =5, $P < 0.05$) and suppressed spontaneous Ca^{2+} wave frequency in the NCX KO SAN cells by 66.2 $\pm$ 13.8% (Fig. 5*C* and *D*; n =6, $P < 0.05$). This included 3 of the 5 WT SAN cells in which Ca^{2+} transients were completely abolished by U73122. In contrast, U73343 (1 μM), the inactive analogue of U73122, had no effect on $[Ca^{2+}]_i$ oscillations, confirming that the effect of U73122 was specific (Fig. 5*E* and *F*, n =5).

To confirm that PLC could influence pacing by changing IP_3 levels, we stimulated IP_3 production using the α-1 adrenergic receptor agonist PE (10 μM). PE activates the Gq-PLC pathway (Scholz *et al.* 1992), which results in downstream generation of IP_3. In WT SAN cells, receptor-mediated stimulation of IP_3 production by PE for 3 min had a positive chronotropic effect on spontaneous Ca^{2+} transients (3.2-fold increase in frequency, Fig. 6*A* and *C*; n =6, $P < 0.05$). The positive chronotropic effect was then blocked by 2-APB (2 μM; Fig. 6*A* and *C*; n =7, $P < 0.05$), underlining the relevance of IP_3 and IP_3R-mediated Ca^{2+} release to this signalling pathway. In NCX KO SAN cells, PE had a similar effect and led to a significant increase (2.2-fold) in the frequency of Ca^{2+} waves that could also be blocked by 2-APB (2 μm; Fig. 6*B* and *D*, n =5, $P < 0.05$). We did not detect any significant changes in Ca^{2+} wave velocities during application of these agents (Fig. 6E; control, 65.15 $\pm$ 2.4; PE, 72.74 $\pm$ 2.97; PE

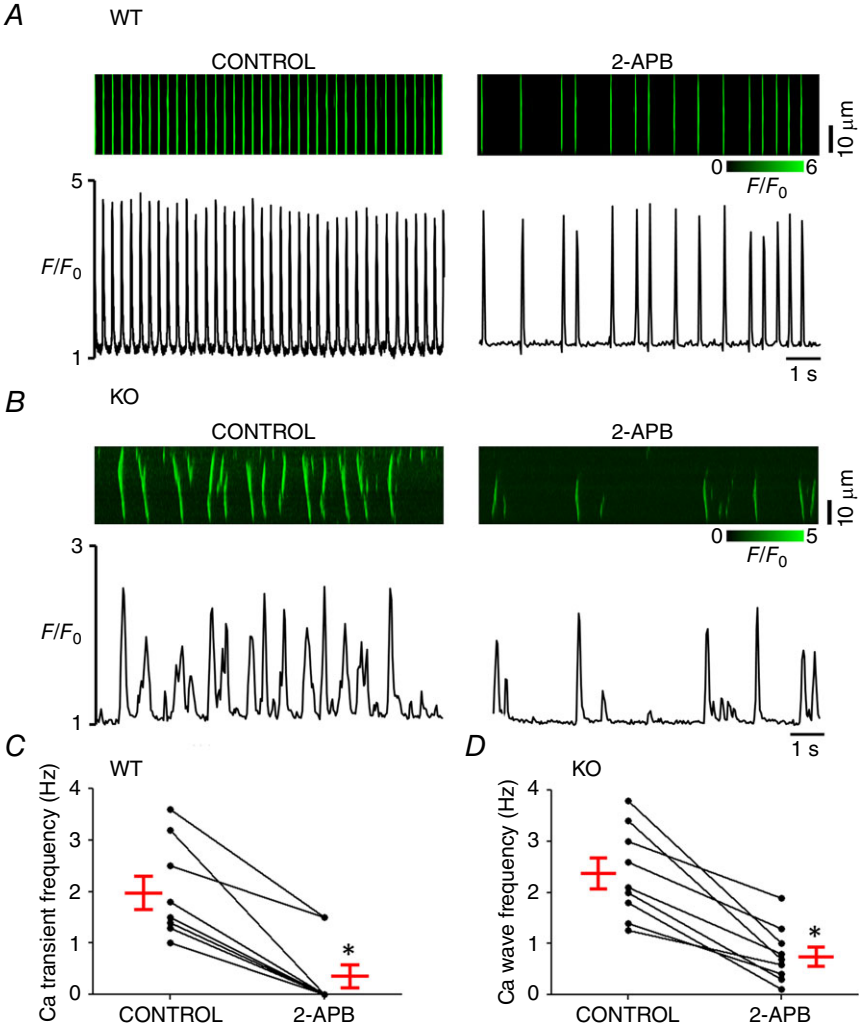

Figure 4. Blocking IP_3Rs inhibits pacing and the Ca^{2+} clock
A and *B*, confocal linescan images and corresponding fluorescence intensity plots of a representative WT (*A*) and an NCX KO SAN cell (*B*) before (CONTROL) and after superfusion with 2-APB (2 μM). *C* and *D*, summary plots showing the effect of 2-APB in nine WT SAN cells (*C*) and in nine NCX KO SAN cells (*D*). $^*P < 0.05$, paired Student's *t*-test.

+ 2-APB, 64.97 ± 2.37 μm s^{-1}; P = n.s.). Thus, while stimulating or inhibiting IP$_3$R-mediated Ca^{2+} release can alter Ca^{2+} transient or wave frequency, it does not alter the velocity of Ca^{2+} wave propagation through the cell.

IP$_3$ signalling in the presence of RyR blockers

IP$_3$Rs could influence pacemaker activity either (1) directly by releasing Ca^{2+} in close proximity to NCX, thereby generating inward NCX current (I_{NCX}) to depolarize the cell, or (2) indirectly by triggering neighbouring RyRs to release Ca^{2+} to activate inward I_{NCX}. Our results in NCX KO cells, which do not depolarize spontaneously, clearly demonstrate that NCX-induced depolarization by IP$_3$R-mediated Ca^{2+} release is not necessary for IP$_3$ to modulate Ca^{2+} wave (e.g. Ca^{2+} clock) frequency (Figs 4*D*, 5*D* and 6*D*). To further study the role of RyRs in the mechanism of IP$_3$-mediated modulation of the Ca^{2+} clock, we recorded Ca^{2+} transients during application of PE (10 μM) while blocking RyRs using Ry (at a blocking concentration of 100 μM to avoid depleting SR Ca^{2+} stores). In WT SAN cells Ry blocked spontaneous Ca^{2+} transients in all five cells tested, and prevented PE from restoring them (Fig. 7). Caffeine-induced Ca^{2+} transients recorded at the end of the protocol indicated that SR Ca^{2+} was not depleted (Fig. 7). Similar results were obtained in NCX KO SAN cells where blocking RyRs

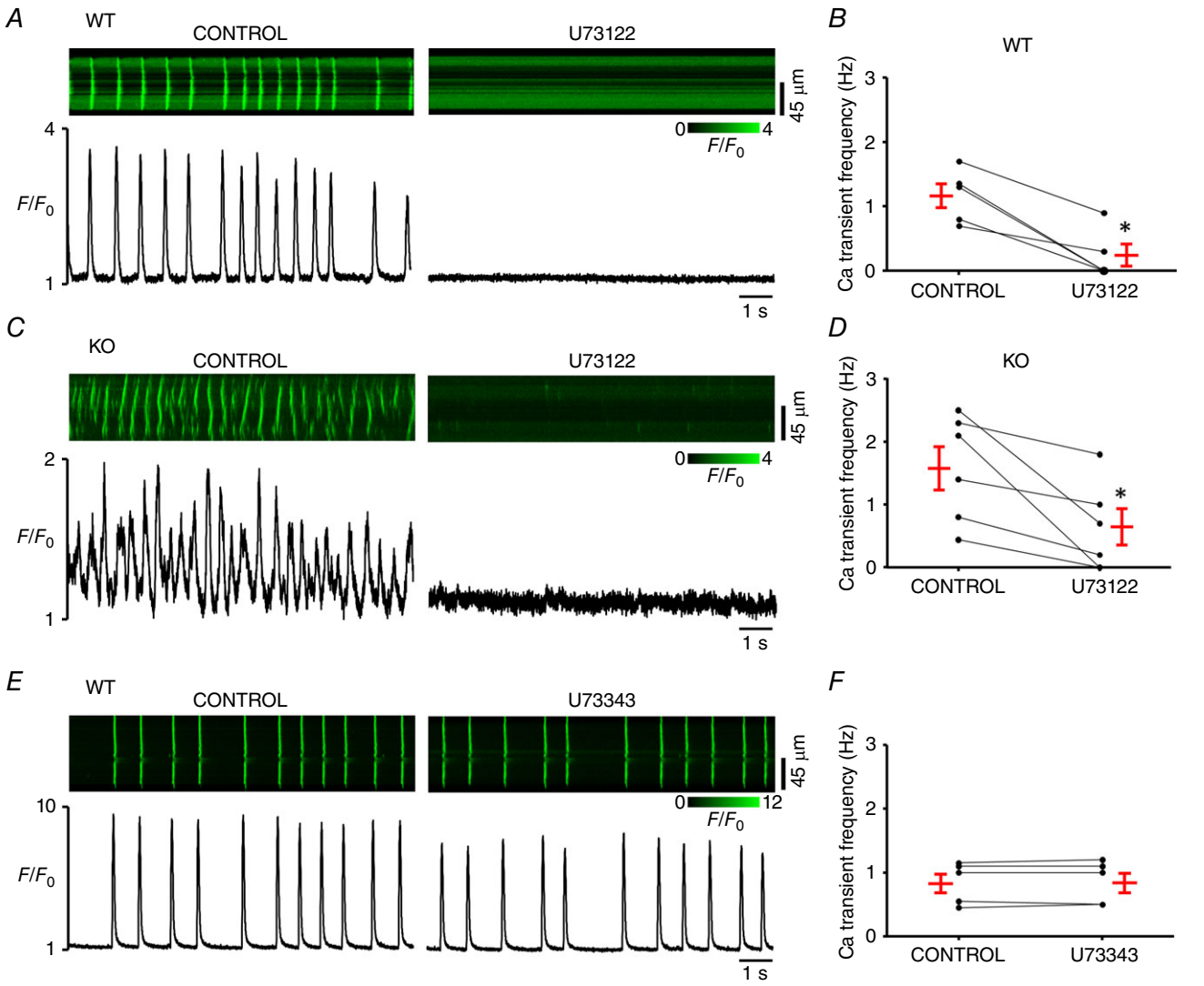

Figure 5. Blocking PLC inhibits pacing and the Ca^{2+} clock
A and *C*, confocal linescan images and corresponding fluorescence intensity plots of a representative WT (*A*) and an NCX KO SAN cell (*C*) before (CONTROL) and after superfusion with the PLC blocker U73122 (1 μM). *B* and *D*, summary plots showing the effects of U73122 in WT SAN cells (*B*; n =5) and NCX KO SAN cells (*D*; n =6). *E* and *F*, representative confocal linescans showing that U73343, the inactive analogue of U73122, has no effect on spontaneous Ca^{2+} transients in WT SAN cells (n =5). *P < 0.05, paired Student's t-test.

with TET (1 mM) caused cessation of Ca^{2+} waves, and subsequent addition of PE failed to restore them (data not shown). Taken together, these results are consistent with the hypothesis that IP_3-mediated Ca^{2+} release from IP_3Rs increases the likelihood of SR Ca^{2+} release by RyRs to modulate pacemaker rate.

Modulation of Ca^{2+} sparks by IP_3R-mediated Ca^{2+} release

Spontaneous LCRs by RyRs in SAN cells are thought to trigger depolarization by stimulating forward mode NCX. A single LCR involves several Ca^{2+} sparks fired by neighbouring Ca^{2+} release units via fire–diffuse–fire propagation (Maltsev *et al.* 2011). To further test the hypothesis that IP_3R-mediated Ca^{2+} release induces Ca^{2+} release from RyR channels, we examined how Ca^{2+} sparks in WT and NCX KO SAN cells are influenced by IP_3 signalling. We observed localized Ca^{2+} release events with characteristics of Ca^{2+} sparks (Cheng & Lederer, 2008) in 47% (86 out of 184 cells) of WT and 56% (65 out of 116 cells) of NCX KO SAN cells. We then tested the effects of IP_3R block on Ca^{2+} sparks in WT (n =6) and NCX KO (n =3) SAN cells. Superfusion of both WT and NCX KO SAN cells with 2-APB resulted in a significant decrease in the frequency and amplitude, but not width or duration, of the Ca^{2+} sparks (Fig. 8).

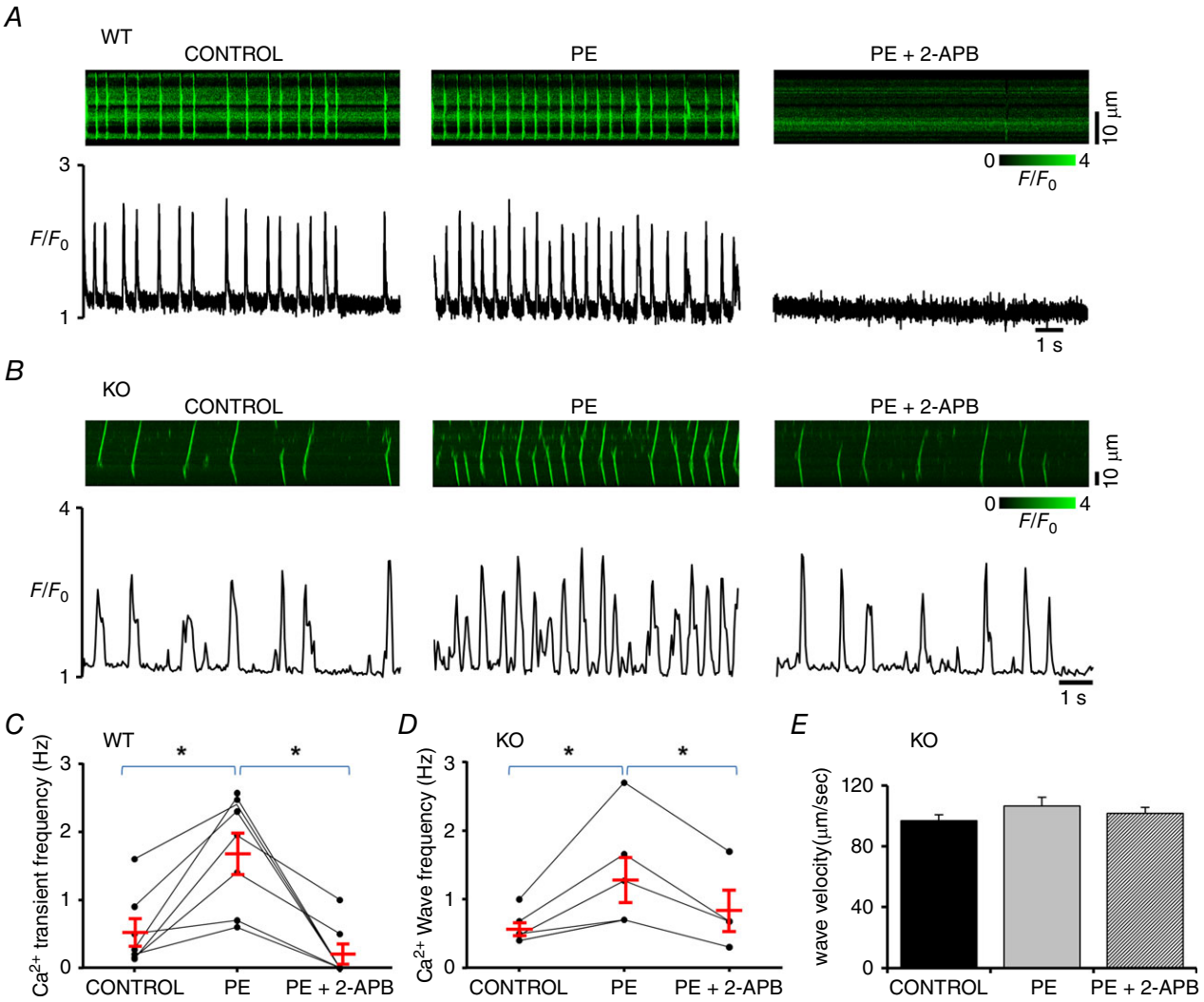

Figure 6. Stimulating IP_3 production accelerates pacing and the Ca^{2+} clock
A and *B*, confocal linescan images and corresponding fluorescence intensity plots of a representative WT (*A*) and an NCX KO SAN cell (*B*) before (CONTROL), during subsequent superfusion with phenylephrine (PE, 10 μM), and during superfusion with PE (10 μM) + 2-APB (2 μM). *C* and *D*, summary plots showing the effects of PE and subsequent application of PE +2-APB for WT (*C*; n =7) and NCX KO SAN cells (*D*; n =5). *E*, mean Ca^{2+} wave velocity in NCX KO SAN cells was unchanged by the pharmacological interventions (PE, PE + 2-APB) in comparison to the controls. $^*P < 0.05$, one-way ANOVA with Holm–Sidak's multiple comparisons test.

The reduction in spark amplitude upon superfusion with 2-APB could not be attributed to a change in SR Ca^{2+} content, as caffeine-releasable Ca^{2+} stores were similar before and after application of the drug (Fig. 2*E* and *F*). This suggests instead that blocking IP$_3$Rs decreases RyR P_o (open probability) and thus recruitment of functional RyR Ca^{2+} release units in a couplon (Lukyanenko *et al.* 2000; Cheng & Lederer, 2008; MacQuaide *et al.* 2010; Lee *et al.* 2013).

In contrast to 2-APB, PE increased Ca^{2+} spark frequency after 3 min in WT and NCX KO SAN cells (Fig. 9). Again, this effect was reversed by 2-APB (Fig. 9). These results support the hypothesis that IP$_3$R-mediated Ca^{2+} release participates in the triggering of Ca^{2+} release from RyRs and thus potentiates the 'Ca^{2+} clock' pathway of pacemaking.

Discussion

SAN pacemaker activity is thought to be driven by the coupled activity of two cellular 'clocks': a membrane clock driven by the inward funny current (I_f) through HCN4 channels, and a calcium clock driven by the inward current through NCX (I_{NCX}) in response to local SR calcium release by RyRs (Santoro & Tibbs, 1999; Lakatta *et al.* 2003, 2006, 2010; Vinogradova *et al.* 2005). In the embryonic heart, an alternative signalling pathway involving IP$_3$ has been shown to play a crucial role in pacemaker activity (Mery *et al.* 2005; Kapur & Banach, 2007; Kapoor *et al.* 2014). In the adult heart, IP$_3$Rs release Ca^{2+} from intracellular Ca^{2+} stores and participate in the pathogenesis of both ventricular hypertrophy (Barac *et al.* 2005; Wang *et al.* 2005; Luo *et al.* 2006; Roderick & Bootman, 2007; Harzheim *et al.* 2009; Nakayama *et al.* 2010; Arantes *et al.* 2012) and heart failure (Gutstein & Marks, 1997; Woodcock *et al.* 1998; Guatimosim *et al.* 2002; Fauconnier *et al.* 2005; Harzheim *et al.* 2009; Hohendanner *et al.* 2015). In atrial myocardium, where IP$_3$R expression levels are 6–10 fold higher than ventricle (Lipp *et al.* 2000; Mackenzie *et al.* 2002), IP$_3$ is thought to contribute to EC coupling by 'facilitating' RyR Ca^{2+} release (Zima & Blatter, 2004), although it may also trigger atrial arrhythmias characterized by spontaneous Ca^{2+} waves. The potential of IP$_3$ as a regulator of cardiac pacemaker activity in the adult SAN has been controversial (Ju *et al.* 2011; Vinogradova, 2011). In the current study we clearly show that IP$_3$ signalling can alter the frequency of pacemaking in murine SAN cells. In WT cells, blockers of IP$_3$ production or IP$_3$Rs reduced pacing rate (Figs 4 and 5), whereas stimulating IP$_3$ signalling accelerated it (Fig. 6). Similar effects of these agents on Ca^{2+} wave frequency in NCX KO mice (Figs 4–6) indicate that the mechanism involves changes in Ca^{2+} clock cycle length mediated by IP$_3$R-mediated Ca^{2+} release near RyRs. Finally, our results in NCX KO mice indicate unequivocally that the effect of IP$_3$ signalling on the 'Ca^{2+} clock' does not depend upon NCX-mediated depolarization in direct response to Ca released by IP$_3$Rs.

Unlike ventricular myocytes, where spontaneous RyR-mediated Ca^{2+} release and Ca^{2+} waves are often the consequence of elevated SR Ca^{2+} load (Jiang *et al.* 2004), RyRs in SAN myocytes release SR Ca^{2+} in response to normal SR refilling and content in accordance with the Ca^{2+} clock mechanism (Vinogradova *et al.* 2004, 2005). In WT cells this locally released Ca^{2+} is removed by NCX, which generates a depolarizing inward current contributing to an AP and a corresponding Ca^{2+} transient. Because NCX KO mice lack any mechanism to

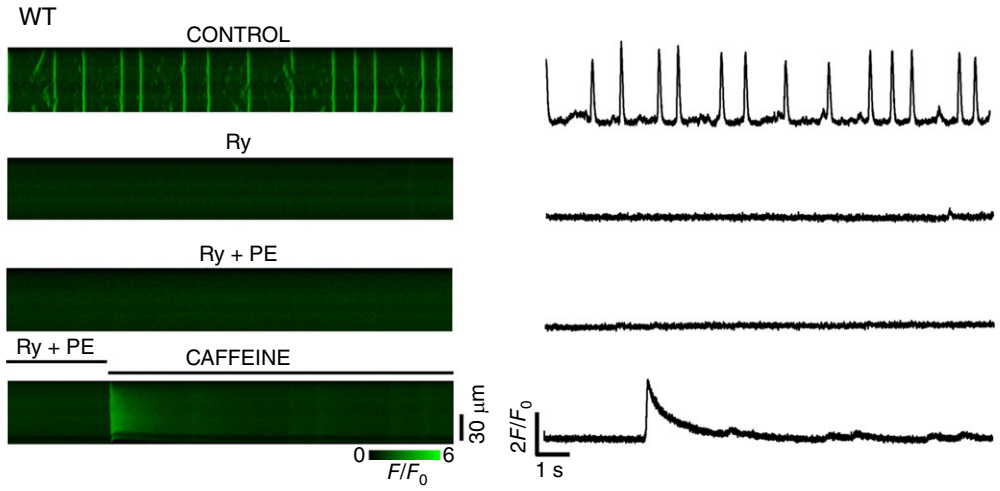

Figure 7. IP$_3$Rs require RyRs to induce pacemaking
Representative confocal linescan images (left) and corresponding fluorescence intensity plots (right) in a WT SAN cell under control conditions (CONTROL), during subsequent superfusion with ryanodine (Ry; 100 μM) alone, and then Ry + phenylephrine (PE; 10 μM). Caffeine (20 mM) was applied at the end of the experiment where indicated by the black line to assess releasable Ca^{2+} in the SR.

remove Ca^{2+} rapidly across the sarcolemma, local Ca^{2+} release from the SR can either (1) facilitate activation of adjacent RyRs and propagate as a Ca^{2+} wave, or (2) fail to propagate and instead generate Ca^{2+} sparks (Groenke *et al.* 2013). Notably the Ca^{2+} waves that occur in NCX KO SAN cells do so even though SR Ca^{2+} content is not significantly increased (Fig. 2*A*–*C*). The lack of SR Ca^{2+} overload despite the absence of NCX is consistent with decreased Ca^{2+} entry through LCCs and increased Ca efflux through the plasma membrane Ca^{2+} pump, which we have shown previously in NCX KO SAN cells (Groenke *et al.* 2013) and NCX KO ventricular myocytes (Pott *et al.* 2005). SAN pacemaker rate can slow down when SR Ca^{2+} load is reduced (Vinogradova *et al.* 2002; Maltsev *et al.* 2011). We found no evidence of SR Ca^{2+} depletion during IP_3R block with 2-APB (Fig. 2*E* and *F*) that could explain the reduction in rate we observed in WT and NCX KO cells. Similar to the reduction in spontaneous pacing rate in WT cells, we observed a decrease in the frequency and amplitude of Ca^{2+} sparks upon blocking IP_3Rs with 2-APB (Fig. 8). Reductions in Ca^{2+} spark frequency are typically attributed to decreases in RyR P_0 (Zima *et al.* 2008). While this can be caused by reductions in SR Ca^{2+} content, drugs that reduce RyR P_o, such as ruthenium red, ryanodine and tetracaine, can also reduce spark frequency without lowering SR Ca^{2+} content (Lukyanenko *et al.* 2000; MacQuaide *et al.* 2010). As SR Ca^{2+} content remained unaffected by 2-APB (Fig. 2*E*

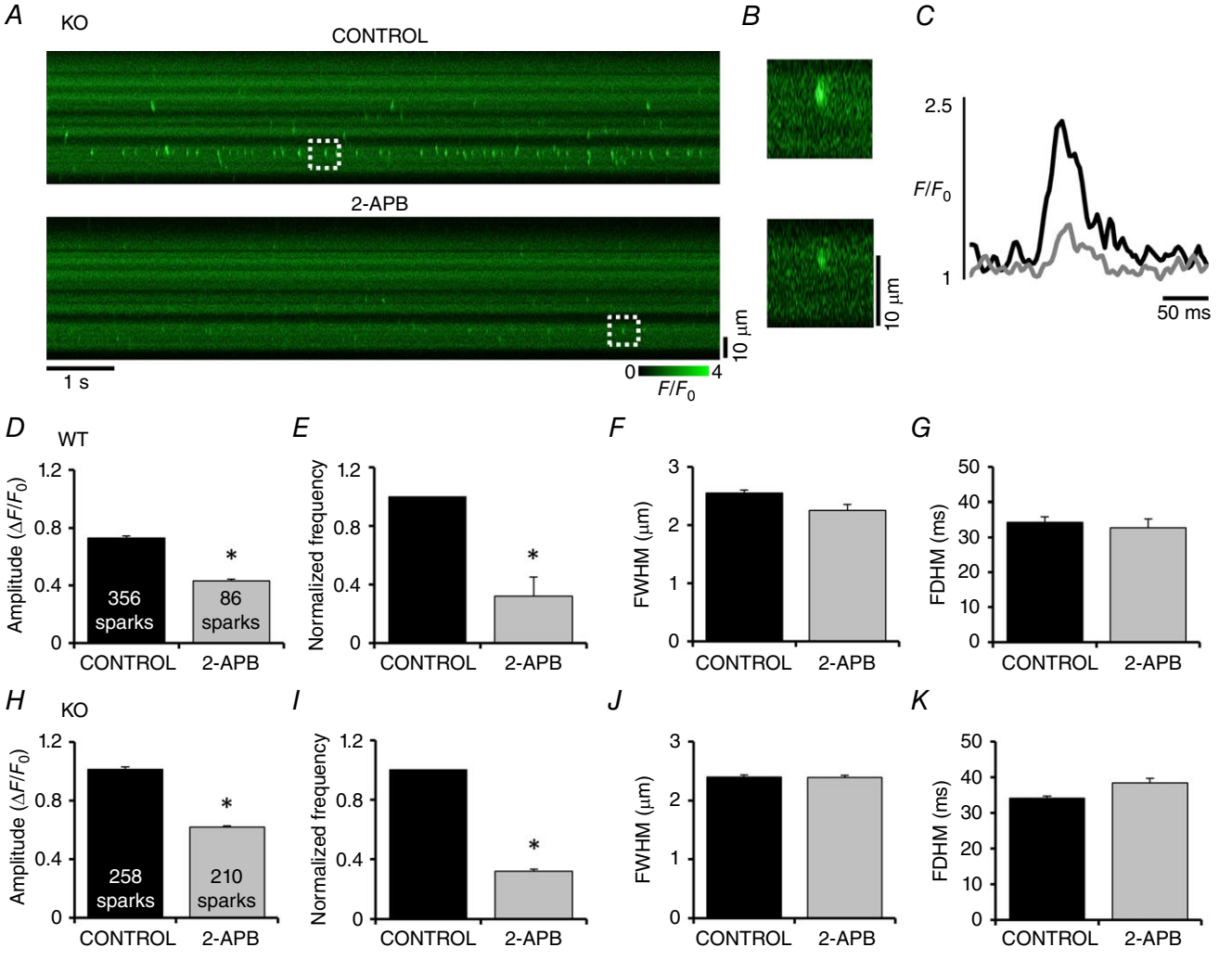

Figure 8. IP_3R-mediated Ca^{2+} release modulates Ca^{2+} Sparks
A, representative confocal linescan images showing Ca^{2+} sparks in an NCX KO SAN cell under control conditions (upper panel) and during superfusion with 2-APB (2 μM; lower panel). *B*, higher magnification images of Ca^{2+} sparks occurring at a single location on the linescan in *A* (indicated by the dotted box) under control conditions (upper) and during superfusion with 2-APB (lower). *C*, fluorescence intensity plots (*black*, control; *grey*, 2-APB) for the sparks shown in *B*. *D*–*K*, summary plots showing the effect of 2-APB on spark amplitude (*D*, *H*), frequency (*E*, *I*), width (*F*, *J*) and duration (*G*, *K*), in WT and KO SAN cells, respectively. $^*P < 0.05$, unpaired Student's *t*-test. FDHM, full duration at half-maximum; FWHM, full width at half-maximum.

and *F*), we conclude that blocking IP$_3$R-mediated Ca^{2+} release decreased the local concentration of Ca^{2+} sensed by RyRs, thereby decreasing RyR P_o and consequently spark amplitude and frequency. Conversely, our data show that Ca^{2+} spark frequency increased after activating the IP$_3$ signalling pathway with PE (Fig. 9). The effect of PE could be blocked with 2-APB, suggesting that the effect was specific for IP$_3$Rs. Taken together, these results are consistent with IP$_3$Rs regulating pacemaker rate through modulation of local Ca^{2+} in the vicinity of RyRs and thus RyR P_o. A similar mechanism has been described to explain how IP$_3$ facilitates EC coupling in atrial myocytes (Zima & Blatter, 2004). The effect is likely to be enhanced in SAN for two reasons: first, SAN cells have higher levels of cAMP in comparison to the rest of the myocardium (Vinogradova *et al.* 2008), and high concentrations of cAMP sensitize IP$_3$Rs to IP$_3$ via a direct effect (Tovey *et al.* 2010; Tovey & Taylor, 2013). Second, IP$_3$Rs are more abundant in atria and the SAN compared to the ventricle (Lipp *et al.* 2000; Mackenzie *et al.* 2002; Ju *et al.* 2011). Thus, it seems likely that IP$_3$Rs of SAN cells are poised to provide a relatively large source of Ca^{2+} to nearby RyRs.

In the present study we were able to slow Ca^{2+} cycling and pacing rate in WT and NCX KO SAN cells using two different blockers of IP$_3$Rs or IP$_3$ production. Blocking or activating PLC could potentially have complicating effects as PLC activation leads to hydrolysis of membrane-associated phosphatidylinositol (4,5)-bisphosphate (PIP_2) into diacylglycerol (DAG) as well as IP$_3$. However, our data show that the effect of PLC activation by PE is blocked by 2-APB (Fig. 6), suggesting that the effect is mediated via IP$_3$ and IP$_3$Rs, as DAG is not known to activate IP$_3$Rs. Our data on Ca^{2+} spark modulation with 2-APB also suggest that there is a basal level of IP$_3$R activity sufficient to provide nearby RyRs with enough Ca^{2+} to trigger their activation. On the other hand, stimulation of IP$_3$ signalling with PE increased the Ca^{2+} cycling rate in WT and KO SAN cells (Fig. 6). PE leads to an increase in intracellular IP$_3$ (Remus *et al.* 2006), which results in Ca^{2+} release by the IP$_3$Rs. We assume that additional Ca^{2+} released by IP$_3$Rs in close proximity to the RyRs could increase their P_0 and thereby increase the 'Ca^{2+} clock' frequency.

Although we found that IP$_3$ signalling could modulate the frequency of Ca^{2+} transients in WT, and Ca^{2+} sparks and waves in KO, we saw no change in the velocity of Ca^{2+} wave propagation in KO upon stimulation or inhibition of IP$_3$Rs (Fig. 6*E*). The reason for this apparent contradiction is not clear, but prior studies in ventricular and atrial cells have shown similar disparities. For example, MacQuaide *et al.* (2010) have shown in permeabilized ventricular myocytes that the RyR blocker ruthenium red can reduce Ca^{2+} wave frequency without retarding wave velocity. A similar phenomenon has been reported in atrial myocytes where block of IP$_3$Rs reduces Ca^{2+} spark frequency but not Ca^{2+} transient propagation velocity from cell periphery to centre (Li *et al.* 2005).

Our results in WT and KO mouse SAN cells are consistent with a report by Ju *et al.* (2011) describing decreased sinus rate in IP$_3$R2 KO mice, although the reduction in rate that we observed with IP$_3$R blockade was much higher. There are several potential explanations for this. First, we conducted our experiments at 20–22°C whereas Ju *et al.* (2011) conducted their experiments at 37°C. The lower temperature we used resulted in a slower and more variable Ca^{2+} transient and wave rate at baseline, and may have increased the sensitivity of our isolated SAN cells to the IP$_3$R blocker. Second, despite the finding that HCN4 expression is unchanged in the IP$_3$R2 KO mice, it is possible that these mice have compensatory adaptations

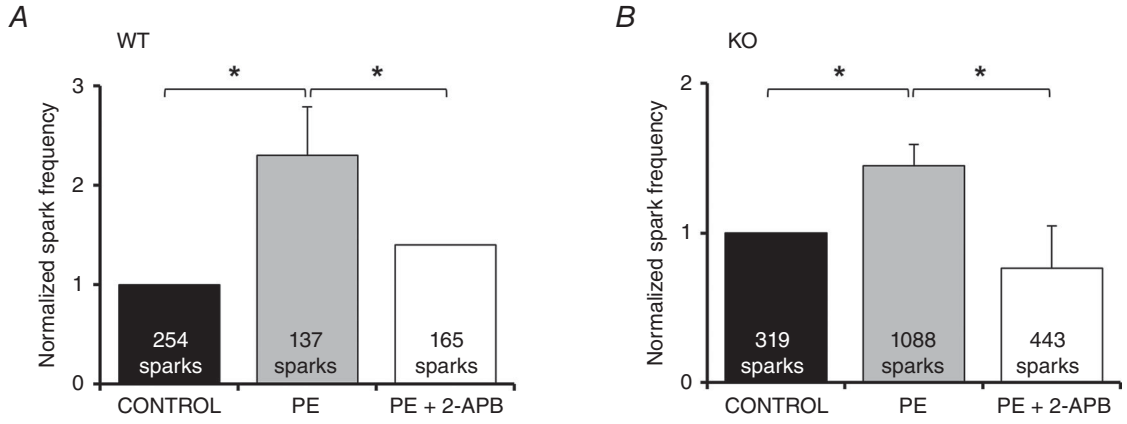

Figure 9. Effect of phenylephrine on Ca^{2+} sparks
A and *B*, summary plots showing the effect of phenylephrine (PE; 10 μM) and the subsequent application of PE (10 μM) + 2-APB (2 μM) on the frequency of Ca^{2+} sparks in WT (*A*) and NCX KO SAN cells (*B*). WT (n =3) and KO cells (n =3) both show an increase in spark frequency upon superfusion with PE that was reduced by subsequent addition of 2-APB. $^*P < 0.05$, one-way ANOVA with Holm–Sidak's multiple comparisons test.

in other membrane channels (e.g. I_{Ca}, I_K, I_{Na}) that might influence and support pacemaker rate in the absence of IP_3R2. Finally, Ju *et al.* (2011) tested the effects of 2-APB on intact SAN tissue preparations whereas we used single SAN cells. It has been our experience that the intact SAN requires higher drug concentrations to achieve the same effect as a lower concentration in single cells. Moreover, it is well known that the SAN is composed of a heterogeneous population of cells with respect to shape, size and electrophysiology and Ca^{2+} handling proteins (Boyett *et al.* 2000; Musa *et al.* 2002; Lancaster *et al.* 2004). In the absence of IP_3R2, it is possible that latent pacemaker cells with less dependence on IP_3 signalling take over to maintain automaticity. We have observed this heterogeneity in our cells with regard to sensitivity to the IP_3R blocker, 2-APB. In 7 of 9 cells, spontaneous Ca^{2+} transients were completely abolished by 2-APB while in the 2 others 2-APB only slowed the rate (see Fig. 4*C*).

Limitations

At high concentrations, 2-APB is known to have non-specific effects in addition to blocking IP_3Rs (Wilcox *et al.* 1998; Bootman *et al.* 2002). However, we used a low concentration (2 μM) that does not have any detectable effect on the amplitude or duration of electrically evoked Ca^{2+} transients in isolated ventricular myocytes (Peppiatt *et al.* 2003; Kapur & Banach, 2007). Thus, the concentration that we used should have minimal off-target effects. Furthermore, we used alternative methods of accessing the IP_3 signalling system, including PE and U73122, which yielded consistent effects. We did not use IP_3R blockers such as xestospongin C (Oka *et al.* 2002), as they clearly inhibit voltage-dependent Ca^{2+} and K^+ currents (Ozaki *et al.* 2002) as well as SR calcium transport ATPase (SERCA) (Castonguay & Robitaille, 2002) at concentrations used to inhibit IP_3Rs.

Conclusion

Our findings support the hypothesis (Bramich *et al.* 2001; Ju *et al.* 2011, 2012) that functional cross-talk between IP_3Rs and RyRs provides a secondary mechanism of SAN pacemaker regulation. Based on our results in NCX KO cells, we also conclude that NCX is not required for IP_3Rs to modulate Ca^{2+} cycling, and thus 'Ca^{2+} clock' frequency. Thus, we suggest that IP_3R-mediated SAN pacemaker regulation is controlled primarily by the Ca^{2+} clock rather than the membrane clock. As has been suggested previously (Ju *et al.* 2011, 2012), IP_3R-mediated pacemaker regulation could have particular importance in the setting of heart failure where IP_3R expression in the SAN is increased (Yanni *et al.* 2011) and HCN4 expression is decreased (Verkerk *et al.* 2003; Zicha *et al.* 2005). Therefore, our findings may support the development of innovative strategies for using modulators of IP_3 signalling to regulate heart rate in failing hearts where IP_3Rs are increased. Given that IP_3Rs are broadly expressed in the heart, further study is needed to address this possibility.

References

Abramochkin DV & Vornanen M (2014). Inhibition of the cardiac ATP-dependent potassium current by KB-R7943. *Comp Biochem Physiol A Mol Integr Physiol* **175**, 38–45.

Arantes LA, Aguiar CJ, Amaya MJ, Figueiro NC, Andrade LM, Rocha-Resende C, Resende RR, Franchini KG, Guatimosim S & Leite MF (2012). Nuclear inositol 1,4,5-trisphosphate is a necessary and conserved signal for the induction of both pathological and physiological cardiomyocyte hypertrophy. *J Mol Cell Cardiol* **53**, 475–486.

Barac YD, Zeevi-Levin N, Yaniv G, Reiter I, Milman F, Shilkrut M, Coleman R, Abassi Z & Binah O (2005). The 1,4,5-inositol trisphosphate pathway is a key component in Fas-mediated hypertrophy in neonatal rat ventricular myocytes. *Cardiovasc Res* **68**, 75–86.

Bootman MD, Collins TJ, Mackenzie L, Roderick HL, Berridge MJ & Peppiatt CM (2002). 2-Aminoethoxydiphenyl borate (2-APB) is a reliable blocker of store-operated Ca^{2+} entry but an inconsistent inhibitor of InsP3-induced Ca^{2+} release. *FASEB J* **16**, 1145–1150.

Boyett MR, Honjo H & Kodama I (2000). The sinoatrial node, a heterogeneous pacemaker structure. *Cardiovasc Res* **47**, 658–687.

Bramich NJ, Cousins HM, Edwards FR & Hirst GD (2001). Parallel metabotropic pathways in the heart of the toad, *Bufo marinus*. *Am J Physiol Heart Circ Physiol* **281**, H1771–1777.

Brustovetsky T, Brittain MK, Sheets PL, Cummins TR, Pinelis V & Brustovetsky N (2011). KB-R7943, an inhibitor of the reverse Na^+/Ca^{2+} exchanger, blocks *N*-methyl-D-aspartate receptor and inhibits mitochondrial complex I. *Br J Pharmacol* **162**, 255–270.

Castonguay A & Robitaille R (2002). Xestospongin C is a potent inhibitor of SERCA at a vertebrate synapse. *Cell Calcium* **32**, 39–47.

Chantawansri C, Huynh N, Yamanaka J, Garfinkel A, Lamp ST, Inoue M, Bridge JH & Goldhaber JI (2008). Effect of metabolic inhibition on couplon behavior in rabbit ventricular myocytes. *Biophys J* **94**, 1656–1666.

Cheng H & Lederer WJ (2008). Calcium sparks. *Physiol Rev* **88**, 1491–1545.

DiFrancesco D (1995). The pacemaker current (I_f) plays an important role in regulating SA node pacemaker activity. *Cardiovasc Res* **30**, 307–308.

Fauconnier J, Lanner JT, Zhang SJ, Tavi P, Bruton JD, Katz A & Westerblad H (2005). Insulin and inositol 1,4,5-trisphosphate trigger abnormal cytosolic Ca^{2+} transients and reveal mitochondrial Ca^{2+} handling defects in cardiomyocytes of *ob*/*ob* mice. *Diabetes* **54**, 2375–2381.

Groenke S, Larson ED, Alber S, Zhang R, Lamp ST, Ren X, Nakano H, Jordan MC, Karagueuzian HS, Roos KP, Nakano A, Proenza C, Philipson KD & Goldhaber JI (2013). Complete atrial-specific knockout of sodium–calcium exchange eliminates sinoatrial node pacemaker activity. *PLoS One* **8**, e81633.

Guatimosim S, Dilly K, Santana LF, Saleet Jafri M, Sobie EA & Lederer WJ (2002). Local Ca^{2+} signaling and EC coupling in heart: Ca^{2+} sparks and the regulation of the $[Ca^{2+}]_i$ transient. *J Mol Cell Cardiol* **34**, 941–950.

Gutstein DE & Marks AR (1997). Role of inositol 1,4,5-trisphosphate receptors in regulating apoptotic signaling and heart failure. *Heart Vessels* Suppl 12, 53–57.

Harzheim D, Movassagh M, Foo RS, Ritter O, Tashfeen A, Conway SJ, Bootman MD & Roderick HL (2009). Increased InsP3Rs in the junctional sarcoplasmic reticulum augment Ca^{2+} transients and arrhythmias associated with cardiac hypertrophy. *Proc Natl Acad Sci U S A* **106**, 11406–11411.

Herrmann S, Lipp P, Wiesen K, Stieber J, Nguyen H, Kaiser E & Ludwig A (2013). The cardiac sodium–calcium exchanger NCX1 is a key player in the initiation and maintenance of a stable heart rhythm. *Cardiovasc Res* **99**, 780–788.

Hohendanner F, Walther S, Maxwell JT, Kettlewell S, Awad S, Smith GL, Lonchyna VA & Blatter LA (2015). Inositol-1,4,5-trisphosphate induced Ca^{2+} release and excitation–contraction coupling in atrial myocytes from normal and failing hearts. *J Physiol* **593**, 1459–1477.

Jiang D, Xiao B, Yang D, Wang R, Choi P, Zhang L, Cheng H & Chen SR (2004). RyR2 mutations linked to ventricular tachycardia and sudden death reduce the threshold for store-overload-induced Ca^{2+} release (SOICR). *Proc Natl Acad Sci U S A* **101**, 13062–13067.

Ju YK, Liu J, Lee BH, Lai D, Woodcock EA, Lei M, Cannell MB & Allen DG (2011). Distribution and functional role of inositol 1,4,5-trisphosphate receptors in mouse sinoatrial node. *Circ Res* **109**, 848–857.

Ju YK, Woodcock EA, Allen DG & Cannell MB (2012). Inositol 1,4,5-trisphosphate receptors and pacemaker rhythms. *J Mol Cell Cardiol* **53**, 375–381.

Kapoor N, Maxwell JT, Mignery GA, Will D, Blatter LA & Banach K (2014). Spatially defined InsP3-mediated signaling in embryonic stem cell-derived cardiomyocytes. *PLoS One* **9**, e83715.

Kapur N & Banach K (2007). Inositol-1,4,5-trisphosphate-mediated spontaneous activity in mouse embryonic stem cell-derived cardiomyocytes. *J Physiol* **581**, 1113–1127.

Lakatta EG, Maltsev VA, Bogdanov KY, Stern MD & Vinogradova TM (2003). Cyclic variation of intracellular calcium: a critical factor for cardiac pacemaker cell dominance. *Circ Res* **92**, e45-50.

Lakatta EG, Maltsev VA & Vinogradova TM (2010). A coupled SYSTEM of intracellular Ca^{2+} clocks and surface membrane voltage clocks controls the timekeeping mechanism of the heart's pacemaker. *Circ Res* **106**, 659–673.

Lakatta EG, Vinogradova T, Lyashkov A, Sirenko S, Zhu W, Ruknudin A & Maltsev VA (2006). The integration of spontaneous intracellular Ca^{2+} cycling and surface membrane ion channel activation entrains normal automaticity in cells of the heart's pacemaker. *Ann N Y Acad Sci* **1080**, 178–206.

Lancaster MK, Jones SA, Harrison SM & Boyett MR (2004). Intracellular Ca^{2+} and pacemaking within the rabbit sinoatrial node: heterogeneity of role and control. *J Physiol* **556**, 481–494.

Lee YS, Liu OZ, Hwang HS, Knollmann BC & Sobie EA (2013). Parameter sensitivity analysis of stochastic models provides insights into cardiac calcium sparks. *Biophys J* **104**, 1142–1150.

Li X, Zima AV, Sheikh F, Blatter LA & Chen J (2005). Endothelin-1-induced arrhythmogenic Ca^{2+} signaling is abolished in atrial myocytes of inositol-1,4,5-trisphosphate(IP3)-receptor type 2-deficient mice. *Circ Res* **96**, 1274–1281.

Lipp P, Laine M, Tovey SC, Burrell KM, Berridge MJ, Li W & Bootman MD (2000). Functional InsP3 receptors that may modulate excitation–contraction coupling in the heart. *Curr Biol* **10**, 939–942.

Lipsius SL & Bers DM (2003). Cardiac pacemaking: I_f vs. Ca^{2+}, is it really that simple? *J Mol Cell Cardiol* **35**, 891–893.

Lipsius SL, Huser J & Blatter LA (2001). Intracellular Ca^{2+} release sparks atrial pacemaker activity. *News Physiol Sci* **16**, 101–106.

Lukyanenko V, Gyorke I, Subramanian S, Smirnov A, Wiesner TF & Gyorke S (2000). Inhibition of Ca^{2+} sparks by ruthenium red in permeabilized rat ventricular myocytes. *Biophys J* **79**, 1273–1284.

Luo DL, Gao J, Lan XM, Wang G, Wei S, Xiao RP & Han QD (2006). Role of inositol 1,4,5-trisphosphate receptors in α1-adrenergic receptor-induced cardiomyocyte hypertrophy. *Acta Pharmacol Sin* **27**, 895–900.

Mackenzie L, Bootman MD, Laine M, Berridge MJ, Thuring J, Holmes A, Li WH & Lipp P (2002). The role of inositol 1,4,5-trisphosphate receptors in Ca^{2+} signalling and the generation of arrhythmias in rat atrial myocytes. *J Physiol* **541**, 395–409.

MacQuaide N, Ramay HR, Sobie EA & Smith GL (2010). Differential sensitivity of Ca^{2+} wave and Ca^{2+} spark events to ruthenium red in isolated permeabilised rabbit cardiomyocytes. *J Physiol* **588**, 4731–4742.

Maltsev AV, Maltsev VA, Mikheev M, Maltseva LA, Sirenko SG, Lakatta EG & Stern MD (2011). Synchronization of stochastic Ca^{2+} release units creates a rhythmic Ca^{2+} clock in cardiac pacemaker cells. *Biophys J* **100**, 271–283.

Mery A, Aimond F, Menard C, Mikoshiba K, Michalak M & Puceat M (2005). Initiation of embryonic cardiac pacemaker activity by inositol 1,4,5-trisphosphate-dependent calcium signaling. *Mol Biol Cell* **16**, 2414–2423.

Musa H, Lei M, Honjo H, Jones SA, Dobrzynski H, Lancaster MK, Takagishi Y, Henderson Z, Kodama I & Boyett MR (2002). Heterogeneous expression of Ca^{2+} handling proteins in rabbit sinoatrial node. *J Histochem Cytochem* **50**, 311–324.

Nakayama H, Bodi I, Maillet M, DeSantiago J, Domeier TL, Mikoshiba K, Lorenz JN, Blatter LA, Bers DM & Molkentin JD (2010). The IP_3 receptor regulates cardiac hypertrophy in response to select stimuli. *Circ Res* **107**, 659–666.

Oka T, Sato K, Hori M, Ozaki H & Karaki H (2002). Xestospongin C, a novel blocker of IP_3 receptor, attenuates the increase in cytosolic calcium level and degranulation that is induced by antigen in RBL-2H3 mast cells. *Br J Pharmacol* **135**, 1959–1966.

Ozaki H, Hori M, Kim YS, Kwon SC, Ahn DS, Nakazawa H, Kobayashi M & Karaki H (2002). Inhibitory mechanism of xestospongin-C on contraction and ion channels in the intestinal smooth muscle. *Br J Pharmacol* **137**, 1207–1212.

Peppiatt CM, Collins TJ, Mackenzie L, Conway SJ, Holmes AB, Bootman MD, Berridge MJ, Seo JT & Roderick HL (2003). 2-Aminoethoxydiphenyl borate (2-APB) antagonises inositol 1,4,5-trisphosphate-induced calcium release, inhibits calcium pumps and has a use-dependent and slowly reversible action on store-operated calcium entry channels. *Cell Calcium* **34**, 97–108.

Picht E, Zima AV, Blatter LA & Bers DM (2007). SparkMaster: automated calcium spark analysis with ImageJ. *Am J Physiol Cell Physiol* **293**, C1073–1081.

Pott C, Philipson KD & Goldhaber JI (2005). Excitation–contraction coupling in Na^+–Ca^{2+} exchanger knockout mice: reduced transsarcolemmal Ca^{2+} flux. *Circ Res* **97**, 1288–1295.

Remus TP, Zima AV, Bossuyt J, Bare DJ, Martin JL, Blatter LA, Bers DM & Mignery GA (2006). Biosensors to measure inositol 1,4,5-trisphosphate concentration in living cells with spatiotemporal resolution. *J Biol Chem* **281**, 608–616.

Reuter H, Henderson SA, Han T, Matsuda T, Baba A, Ross RS, Goldhaber JI & Philipson KD (2002). Knockout mice for pharmacological screening: testing the specificity of Na^+–Ca^{2+} exchange inhibitors. *Circ Res* **91**, 90–92.

Roderick HL & Bootman M (2007). Pacemaking, arrhythmias, inotropy and hypertrophy; the many possible facets of InsP3 signalling in cardiac myocytes. *J Physiol* **581**, 883–884.

Santoro B & Tibbs GR (1999). The HCN gene family: molecular basis of the hyperpolarization-activated pacemaker channels. *Ann N Y Acad Sci* **868**, 741–764.

Schneider CA, Rasband WS & Eliceiri KW (2012). NIH Image to ImageJ: 25 years of image analysis. *Nature Methods* **9**, 671–675.

Scholz J, Troll U, Sandig P, Schmitz W, Scholz H & Schulte Am Esch J (1992). Existence and α1-adrenergic stimulation of inositol polyphosphates in mammalian heart. *Mol Pharmacol* **42**, 134–140.

Tada M, Takeuchi A, Hashizume M, Kitamura K & Kano M (2014). A highly sensitive fluorescent indicator dye for calcium imaging of neural activity *in vitro* and *in vivo*. *Eur J Neurosci* **39**, 1720–1728.

Tovey SC, Dedos SG, Rahman T, Taylor EJ, Pantazaka E & Taylor CW (2010). Regulation of inositol 1,4,5-trisphosphate receptors by cAMP independent of cAMP-dependent protein kinase. *J Biol Chem* **285**, 12979–12989.

Tovey SC & Taylor CW (2013). Cyclic AMP directs inositol (1,4,5)-trisphosphate-evoked Ca^{2+} signalling to different intracellular Ca^{2+} stores. *J Cell Sci* **126**, 2305–2313.

Verkerk AO, Wilders R, Coronel R, Ravesloot JH & Verheijck EE (2003). Ionic remodeling of sinoatrial node cells by heart failure. *Circulation* **108**, 760–766.

Vinogradova TM, Bogdanov KY & Lakatta EG (2002). β-Adrenergic stimulation modulates ryanodine receptor Ca^{2+} release during diastolic depolarization to accelerate pacemaker activity in rabbit sinoatrial nodal cells. *Circ Res* **90**, 73–79.

Vinogradova TM, Lakatta EG (2011). Basal phospholipase C (PLC) activation is obligatory for cardiac pacemaker activity. *Biophys J* **100**, 517*a*–517*a*.

Vinogradova TM, Lyashkov AE, Zhu W, Ruknudin AM, Sirenko S, Yang D, Deo S, Barlow M, Johnson S, Caffrey JL, Zhou YY, Xiao RP, Cheng H, Stern MD, Maltsev VA & Lakatta EG (2006). High basal protein kinase A-dependent phosphorylation drives rhythmic internal Ca^{2+} store oscillations and spontaneous beating of cardiac pacemaker cells. *Circ Res* **98**, 505–514.

Vinogradova TM, Maltsev VA, Bogdanov KY, Lyashkov AE & Lakatta EG (2005). Rhythmic Ca^{2+} oscillations drive sinoatrial nodal cell pacemaker function to make the heart tick. *Ann N Y Acad Sci* **1047**, 138–156.

Vinogradova TM, Sirenko S, Lyashkov AE, Younes A, Li Y, Zhu W, Yang D, Ruknudin AM, Spurgeon H & Lakatta EG (2008). Constitutive phosphodiesterase activity restricts spontaneous beating rate of cardiac pacemaker cells by suppressing local Ca^{2+} releases. *Circ Res* **102**, 761–769.

Vinogradova TM, Zhou YY, Maltsev V, Lyashkov A, Stern M & Lakatta EG (2004). Rhythmic ryanodine receptor Ca^{2+} releases during diastolic depolarization of sinoatrial pacemaker cells do not require membrane depolarization. *Circ Res* **94**, 802–809.

Wang H, Oestreich EA, Maekawa N, Bullard TA, Vikstrom KL, Dirksen RT, Kelley GG, Blaxall BC & Smrcka AV (2005). Phospholipase C ε modulates β-adrenergic receptor-dependent cardiac contraction and inhibits cardiac hypertrophy. *Circ Res* **97**, 1305–1313.

Wiczer BM, Marcu R & Hawkins BJ (2014). KB-R7943, a plasma membrane Na^+/Ca^{2+} exchanger inhibitor, blocks opening of the mitochondrial permeability transition pore. *Biochem Biophys Res Commun* **444**, 44–49.

Wilcox RA, Primrose WU, Nahorski SR & Challiss RA (1998). New developments in the molecular pharmacology of the myo-inositol 1,4,5-trisphosphate receptor. *Trends Pharmacol Sci* **19**, 467–475.

Woodcock EA, Matkovich SJ & Binah O (1998). Ins(1,4,5)P3 and cardiac dysfunction. *Cardiovasc Res* **40**, 251–256.

Yanni J, Tellez JO, Maczewski M, Mackiewicz U, Beresewicz A, Billeter R, Dobrzynski H & Boyett MR (2011). Changes in ion channel gene expression underlying heart failure-induced sinoatrial node dysfunction. *Circ Heart Fail* **4**, 496–508.

Zicha S, Fernandez-Velasco M, Lonardo G, L'Heureux N & Nattel S (2005). Sinus node dysfunction and hyperpolarization-activated (HCN) channel subunit remodeling in a canine heart failure model. *Cardiovasc Res* **66**, 472–481.

Zima AV & Blatter LA (2004). Inositol-1,4,5-trisphosphate-dependent Ca^{2+} signalling in cat atrial excitation–contraction coupling and arrhythmias. *J Physiol* **555**, 607–615.

Zima AV, Picht E, Bers DM & Blatter LA (2008). Partial inhibition of sarcoplasmic reticulum ca release evokes long-lasting Ca release events in ventricular myocytes: role of luminal Ca in termination of Ca release. *Biophys J* **94**, 1867–1879.

Additional information

Competing interests

None declared.

Author contributions

Conception and design of the experiments: N.K., K.D.P., J.I.G. Collection, analysis and interpretation of data: N.K., A.T., J.K., R.Z., K.D.P., J.I.G. Drafting the article: N.K., K.D.P., J.I.G. All authors have approved the final version of the manuscript.

Funding

This work was supported by National Institutes of Health grants R01 HL048509 to J.I.G. and K.D.P., R01 HL070828 to J.I.G. and the Dorothy and E. Phillip Lyon Chair for Laser Research to J.I.G.